Supplement

Table S1: Running EPS in RWI series. Bold font: periods showing a stabilized EPS > 0.85. Abbreviations: Start year: the first year in the window; End year: the last year in the window; N cores: the number of cores; N trees: the number of trees; N corr: total number of correlations as number of within-tree + between-tree correlations computed; Rbar: mean of all the correlations between different cores; EPS: Expressed Population Signal; SNR: Signal-to-Noise Ratio.

Start year	End year	N cores	N trees	N corr	Rbar	EPS	SNR
1559	1588	12	12	15	0.197	0.596	1.475
1574	1603	17	17	36	0.207	0.702	2.353
1589	1618	22	22	66	0.212	0.763	3.227
1604	1633	26	26	136	0.131	0.719	2.560
1619	1648	30	30	231	0.210	0.854	5.846
1634	1663	34	34	325	0.161	0.833	5.001
1649	**1678**	**39**	**39**	**435**	**0.175**	**0.864**	**6.348**
1664	**1693**	**43**	**43**	**561**	**0.277**	**0.929**	**13.034**
1679	**1708**	**45**	**45**	**741**	**0.264**	**0.933**	**13.955**
1694	**1723**	**45**	**45**	**946**	**0.209**	**0.921**	**11.594**
1709	**1738**	**46**	**46**	**990**	**0.216**	**0.925**	**12.388**
1724	**1753**	**51**	**51**	**990**	**0.240**	**0.934**	**14.219**
1739	**1768**	**54**	**54**	**1035**	**0.216**	**0.927**	**12.644**
1754	**1783**	**59**	**59**	**1275**	**0.245**	**0.943**	**16.552**
1769	**1798**	**64**	**64**	**1431**	**0.298**	**0.958**	**22.900**
1784	**1813**	**70**	**70**	**1711**	**0.233**	**0.947**	**17.907**
1799	**1828**	**72**	**72**	**2016**	**0.238**	**0.952**	**20.040**
1814	**1843**	**76**	**76**	**2346**	**0.194**	**0.943**	**16.566**
1829	**1858**	**80**	**80**	**2556**	**0.190**	**0.944**	**16.936**
1844	**1873**	**86**	**86**	**2775**	**0.222**	**0.955**	**21.382**
1859	**1888**	**87**	**87**	**3081**	**0.183**	**0.946**	**17.646**
1874	**1903**	**89**	**89**	**3655**	**0.196**	**0.954**	**20.958**
1889	**1918**	**91**	**91**	**3828**	**0.194**	**0.955**	**21.127**
1904	**1933**	**93**	**93**	**3916**	**0.140**	**0.935**	**14.485**
1919	**1948**	**96**	**96**	**4095**	**0.189**	**0.955**	**21.146**
1934	**1963**	**100**	**100**	**4278**	**0.292**	**0.975**	**38.379**
1949	**1978**	**102**	**102**	**4560**	**0.333**	**0.980**	**47.884**
1964	**1993**	**102**	**102**	**5050**	**0.380**	**0.984**	**61.775**
1979	**2008**	**102**	**102**	**5151**	**0.426**	**0.987**	**75.668**
1994	**2023**	**102**	**102**	**45**	**0.372**	**0.856**	**5.935**

Table S2: Running EPS in EWI series. Bold font: periods showing a stabilized EPS > 0.85. Abbreviations: Start year: the first year in the window; End year: the last year in the window; N cores: the number of cores; N trees: the number of trees; N corr: total number of correlations as number of within-tree + between-tree correlations computed; Rbar: mean of all the correlations between different cores; EPS: Expressed Population Signal; SNR: Signal-to-Noise Ratio.

Start year	End year	N cores	N trees	N corr	Rbar	EPS	SNR
1559	1588	12	12	15	0.015	0.085	0.093
1574	1603	17	17	36	0.073	0.415	0.709
1589	1618	22	22	66	0.116	0.611	1.572
1604	1633	26	26	136	0.030	0.347	0.532
1619	1648	30	30	231	0.071	0.626	1.672
1634	1663	34	34	325	0.049	0.572	1.338
1649	1678	39	39	435	0.076	0.712	2.473
1664	1693	43	43	561	0.145	0.852	5.761
1679	1708	45	45	741	0.150	0.873	6.895
1694	1723	45	45	946	0.099	0.829	4.860
1709	1738	46	46	990	0.073	0.779	3.534
1724	1753	51	51	990	0.076	0.786	3.676
1739	1768	54	54	1035	0.086	0.812	4.306
1754	1783	59	59	1275	0.079	0.813	4.358
1769	**1798**	**64**	**64**	**1431**	**0.152**	**0.906**	**9.664**
1784	**1813**	**70**	**70**	**1711**	**0.107**	**0.876**	**7.037**
1799	**1828**	**72**	**72**	**2016**	**0.097**	**0.873**	**6.849**
1814	**1843**	**76**	**76**	**2346**	**0.089**	**0.871**	**6.760**
1829	**1858**	**80**	**80**	**2556**	**0.093**	**0.881**	**7.422**
1844	**1873**	**86**	**86**	**2775**	**0.102**	**0.895**	**8.486**
1859	**1888**	**87**	**87**	**3081**	**0.100**	**0.898**	**8.819**
1874	**1903**	**89**	**89**	**3655**	**0.110**	**0.914**	**10.647**
1889	**1918**	**91**	**91**	**3828**	**0.105**	**0.911**	**10.277**
1904	**1933**	**93**	**93**	**3916**	**0.049**	**0.822**	**4.609**
1919	**1948**	**96**	**96**	**4095**	**0.066**	**0.865**	**6.399**
1934	**1963**	**100**	**100**	**4278**	**0.107**	**0.917**	**11.088**
1949	**1978**	**102**	**102**	**4560**	**0.140**	**0.940**	**15.641**
1964	**1993**	**102**	**102**	**5050**	**0.139**	**0.942**	**16.267**
1979	**2008**	**102**	**102**	**5151**	**0.183**	**0.958**	**22.843**
1994	**2023**	**102**	**102**	**45**	**0.179**	**0.686**	**2.183**

Table S3: Running EPS in LWI series. Bold font: periods showing a stabilized EPS > 0.85. Abbreviations: Start year: the first year in the window; End year: the last year in the window; N cores: the number of cores; N trees: the number of trees; N corr: total number of correlations as number of within-tree + between-tree correlations computed; Rbar: mean of all the correlations between different cores; EPS: Expressed Population Signal; SNR: Signal-to-Noise Ratio.

Start year	End year	N cores	N trees	N corr	Rbar	EPS	SNR
1559	1588	12	12	15	0.182	0.571	1.333
1574	1603	17	17	36	0.202	0.695	2.279
1589	1618	21	21	66	0.182	0.728	2.672
1604	1633	25	25	136	0.158	0.761	3.193
1619	1648	29	29	210	0.198	0.838	5.184
1634	1663	33	33	300	0.177	0.843	5.364
1649	**1678**	**38**	**38**	**406**	**0.213**	**0.887**	**7.843**

1664	**1693**	**42**	**42**	**528**	**0.295**	**0.933**	**13.838**
1679	**1708**	**44**	**44**	**703**	**0.249**	**0.926**	**12.598**
1694	**1723**	**45**	**45**	**903**	**0.196**	**0.913**	**10.506**
1709	**1738**	**46**	**46**	**946**	**0.221**	**0.926**	**12.491**
1724	**1753**	**51**	**51**	**990**	**0.260**	**0.941**	**15.847**
1739	**1768**	**54**	**54**	**1035**	**0.228**	**0.931**	**13.598**
1754	**1783**	**59**	**59**	**1275**	**0.237**	**0.941**	**15.821**
1769	**1798**	**64**	**64**	**1431**	**0.237**	**0.944**	**16.739**
1784	**1813**	**70**	**70**	**1711**	**0.226**	**0.945**	**17.198**
1799	**1828**	**72**	**72**	**2016**	**0.234**	**0.951**	**19.503**
1814	**1843**	**76**	**76**	**2346**	**0.178**	**0.937**	**14.967**
1829	**1858**	**80**	**80**	**2556**	**0.168**	**0.936**	**14.541**
1844	**1873**	**86**	**86**	**2775**	**0.200**	**0.949**	**18.726**
1859	**1888**	**87**	**87**	**3081**	**0.150**	**0.933**	**13.956**
1874	**1903**	**89**	**89**	**3655**	**0.159**	**0.942**	**16.278**
1889	**1918**	**91**	**91**	**3828**	**0.167**	**0.947**	**17.702**
1904	**1933**	**93**	**93**	**3916**	**0.143**	**0.937**	**14.907**
1919	**1948**	**96**	**96**	**4095**	**0.196**	**0.957**	**22.148**
1934	**1963**	**100**	**100**	**4278**	**0.290**	**0.974**	**37.942**
1949	**1978**	**102**	**102**	**4560**	**0.306**	**0.977**	**42.231**
1964	**1993**	**102**	**102**	**5050**	**0.341**	**0.981**	**52.229**
1979	**2008**	**102**	**102**	**5151**	**0.387**	**0.985**	**64.357**
1994	**2023**	**102**	**102**	**45**	**0.452**	**0.892**	**8.236**

Table S4: Influence of pollarding on precipitation signals: results from the RWI linear mixed-effects model. Fixed effects: November–June precipitation (CRU data, 1902–2022) and time since pollarding. Random effects: the individual sampled trees (N = 93); $\sigma^2 = 0.06$. Observations = 6708. Marginal $R^2 = 0.245$; Conditional $R^2 = 0.249$. CI: confidence interval.

Predictors	Estimates	CI	p value
(Intercept)	0.79059	0.66120 – 0.91997	<0.001
pp rwi	0.00088	0.00062 – 0.00114	<0.001
time [1]	-0.09783	-0.28727 – 0.09161	0.311
time [2]	-0.12816	-0.31943 – 0.06310	0.189
time [3]	-0.24495	-0.43954 – -0.05037	0.014
time [4]	-0.36922	-0.56703 – -0.17141	<0.001
time [5]	-0.35584	-0.55709 – -0.15460	0.001
time [6]	-0.14759	-0.33529 – 0.04010	0.123
time [7]	-0.30347	-0.51550 – -0.09143	0.005
time [8]	-0.4105	-0.61363 – -0.20737	<0.001
time [9]	-0.27058	-0.46686 – -0.07430	0.007
time [10]	-0.28611	-0.41948 – -0.15273	<0.001
pp rwi × time [1]	-0.00034	-0.00075 – 0.00008	0.112
pp rwi × time [2]	-0.00061	-0.00103 – -0.00018	0.005
pp rwi × time [3]	-0.00028	-0.00071 – 0.00014	0.194
pp rwi × time [4]	0.00003	-0.00038 – 0.00045	0.881

pp rwi × time [5]	0.00014	-0.00028 – 0.00056	0.511
pp rwi × time [6]	-0.00027	-0.00068 – 0.00013	0.187
pp rwi × time [7]	0.0002	-0.00025 – 0.00066	0.383
pp rwi × time [8]	0.00053	0.00009 – 0.00097	0.018
pp rwi × time [9]	0.00023	-0.00021 – 0.00066	0.303
pp rwi × time [10]	0.00032	0.00005 – 0.00059	0.021

Table S5: Influence of pollarding on precipitation signals: results from the EWI linear-mixed effects model. Fixed effects: November–February precipitation (CRU data, 1902–2022) and time since pollarding. Random effects: the individual sampled trees (N = 93); $\sigma^2 = 0.05$. Observations = 6726. Marginal $R^2 = 0.061$; Conditional $R^2 = 0.062$. CI: confidence interval.

Predictors	Estimates	CI	p value
(Intercept)	0.83659	0.75025 – 0.92294	<0.001
pp ewi	0.00074	0.00039 – 0.00109	<0.001
time [1]	0.03264	-0.09473 – 0.16001	0.615
time [2]	0.03777	-0.08248 – 0.15802	0.538
time [3]	-0.01363	-0.14047 – 0.11321	0.833
time [4]	-0.12094	-0.25491 – 0.01304	0.077
time [5]	-0.08716	-0.22017 – 0.04585	0.199
time [6]	0.05555	-0.07039 – 0.18148	0.387
time [7]	0.03131	-0.10284 – 0.16546	0.647
time [8]	0.00879	-0.12193 – 0.13951	0.895
time [9]	0.03283	-0.09596 – 0.16162	0.617
time [10]	0.04401	-0.04491 – 0.13293	0.332
pp ewi × time [1]	0.00007	-0.00048 – 0.00063	0.791
pp ewi × time [2]	-0.00035	-0.00088 – 0.00017	0.187
pp ewi × time [3]	-0.00028	-0.00083 – 0.00027	0.318
pp ewi × time [4]	0.000003	-0.00055 – 0.00055	0.991
pp ewi × time [5]	0.00006	-0.00048 – 0.00061	0.821
pp ewi × time [6]	-0.00042	-0.00095 – 0.00011	0.123
pp ewi × time [7]	-0.00023	-0.00080 – 0.00034	0.422
pp ewi × time [8]	-0.00008	-0.00064 – 0.00047	0.775
pp ewi × time [9]	-0.00009	-0.00066 – 0.00048	0.76
pp ewi × time [10]	-0.0001	-0.00047 – 0.00026	0.569

Table S6: Influence of pollarding on precipitation signals: results from the LWI linear-mixed effects model. Fixed effects: November–June precipitation (CRU data, 1902–2022) and time since pollarding. Random effects: the individual sampled trees (N = 93); $\sigma^2 = 0.22$. Observations = 6726. Marginal $R^2 = 0.284$; Conditional $R^2 = 0.286$. CI: confidence interval.

Predictors	Estimates	CI	p value
(Intercept)	0.83852	0.59589 – 1.08114	<0.001
pp lwi	0.00158	0.00109 – 0.00207	<0.001
time [1]	-0.40885	-0.76754 – -0.05015	0.025
time [2]	-0.57884	-0.94100 – -0.21669	0.002
time [3]	-0.54786	-0.91571 – -0.18001	0.004

time [4]	-0.78633	-1.15985 – -0.41281	<0.001
time [5]	-0.77853	-1.15880 – -0.39826	<0.001
time [6]	-0.68271	-1.03804 – -0.32738	<0.001
time [7]	-0.87925	-1.28130 – -0.47720	<0.001
time [8]	-1.07826	-1.46238 – -0.69413	<0.001
time [9]	-0.79045	-1.16223 – -0.41868	<0.001
time [10]	-0.84514	-1.09551 – -0.59478	<0.001
pp lwi × time [1]	-0.00091	-0.00170 – -0.00013	0.022
pp lwi × time [2]	-0.00112	-0.00193 – -0.00032	0.006
pp lwi × time [3]	-0.0009	-0.00171 – -0.00009	0.029
pp lwi × time [4]	-0.00007	-0.00085 – 0.00072	0.864
pp lwi × time [5]	0.00011	-0.00068 – 0.00091	0.785
pp lwi × time [6]	-0.00004	-0.00081 – 0.00072	0.91
pp lwi × time [7]	0.00062	-0.00025 – 0.00148	0.16
pp lwi × time [8]	0.00129	0.00046 – 0.00213	0.002
pp lwi × time [9]	0.00056	-0.00026 – 0.00138	0.178
pp lwi × time [10]	0.00082	0.00031 – 0.00133	0.002

Table S7: Correspondence between extreme dry years identified in the reconstructed November–June precipitation series (1649–2023) for northcentral Spain and documentary records. Bold font: Pre-instrumental period.

Extreme dry year	Precipitation (mm)	Documentary record
1683	**250**	***Pro pluvia* rogation in Valladolid performed in April (Bellido Blanco, 2017); Historical drought affecting most of peninsular Spain (Centro de Estudios Hidrográficos, 2013).**
1698	**293**	***Pro pluvia* rogation in Valladolid performed in May (Bellido Blanco, 2017); *Pro pluvia* rogation in Zamora performed in spring (Domínguez-Castro et al., 2010); Historical drought affecting most of peninsular Spain (Centro de Estudios Hidrográficos, 2013).**
1734	**251**	***Pro pluvia* rogation in Valladolid performed in May (Bellido Blanco, 2017); Historical drought affecting Castile, Aragon, and Andalusia (Centro de Estudios Hidrográficos, 2013).**
1737	**284**	***Pro pluvia* rogation in Valladolid performed in April (Bellido Blanco, 2017); *Pro pluvia* rogation in Zamora performed in winter (Domínguez-Castro et al., 2010); Historical drought affecting most of peninsular Spain (Centro de Estudios Hidrográficos, 2013).**
1738	**295**	**Two *pro pluvia* rogations in Valladolid performed in April (Bellido Blanco, 2017); One *pro pluvia* rogation in Zamora performed in winter and another one in spring (Domínguez-Castro et al., 2010); Historical drought affecting most of peninsular Spain (Centro de Estudios Hidrográficos, 2013).**
1775	**284**	**Three *pro pluvia* rogations in Valladolid performed in May (Bellido Blanco, 2017); *Pro pluvia* rogation in Zamora performed in spring (Domínguez-Castro et al., 2012); Historical drought affecting Castile (Centro de Estudios Hidrográficos, 2013).**
1868	**287**	**Two *pro pluvia* rogations in Valladolid performed in April (Bellido Blanco, 2017); Historical drought affecting most of peninsular Spain (Centro de Estudios Hidrográficos, 2013).**

1898	**296**	**Historical drought affecting most of peninsular Spain (Centro de Estudios Hidrográficos, 2013).**
1949	293	Spanish Drought Catalogue (Trullenque-Blanco et al., 2024).
1981	291	Spanish Drought Catalogue (Trullenque-Blanco et al. 2024).
1995	271	Spanish Drought Catalogue (Trullenque-Blanco et al. 2024).
1999	286	Spanish Drought Catalogue (Trullenque-Blanco et al. 2024).
2005	271	Spanish Drought Catalogue (Trullenque-Blanco et al. 2024).
2012	260	Spanish Drought Catalogue (Trullenque-Blanco et al. 2024).

Table S8: Wet and dry periods detected in the reconstructed November–June precipitation series (1649–2023) for northcentral Spain. Bold font: Pre-instrumental period.

Period	Start year	End year	Mean precipitation (mm)	Duration (years)
	1702	**1712**	**463**	**11**
	1719	**1737**	**474**	**19**
	1756	**1769**	**481**	**14**
	1793	**1804**	**464**	**12**
Wet	**1806**	**1818**	**463**	**13**
	1855	**1864**	**459**	**10**
	1924	1938	467	15
	1953	1970	484	18
	1971	1981	456	11
	1652	**1669**	**407**	**18**
	1739	**1756**	**425**	**18**
	1769	**1778**	**429**	**10**
Dry	**1818**	**1842**	**419**	**25**
	1864	**1879**	**429**	**16**
	1881	**1897**	**441**	**17**
	1938	1949	418	12

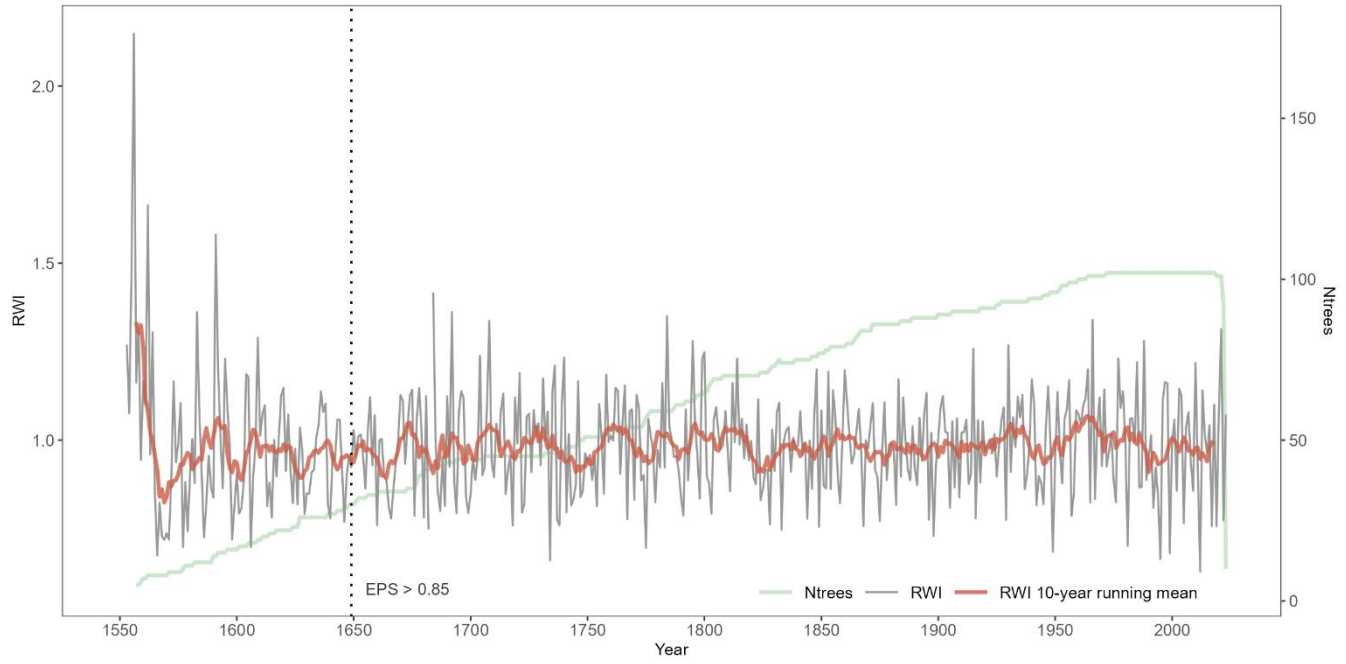

Figure S1: RWI chronology and sample depth.

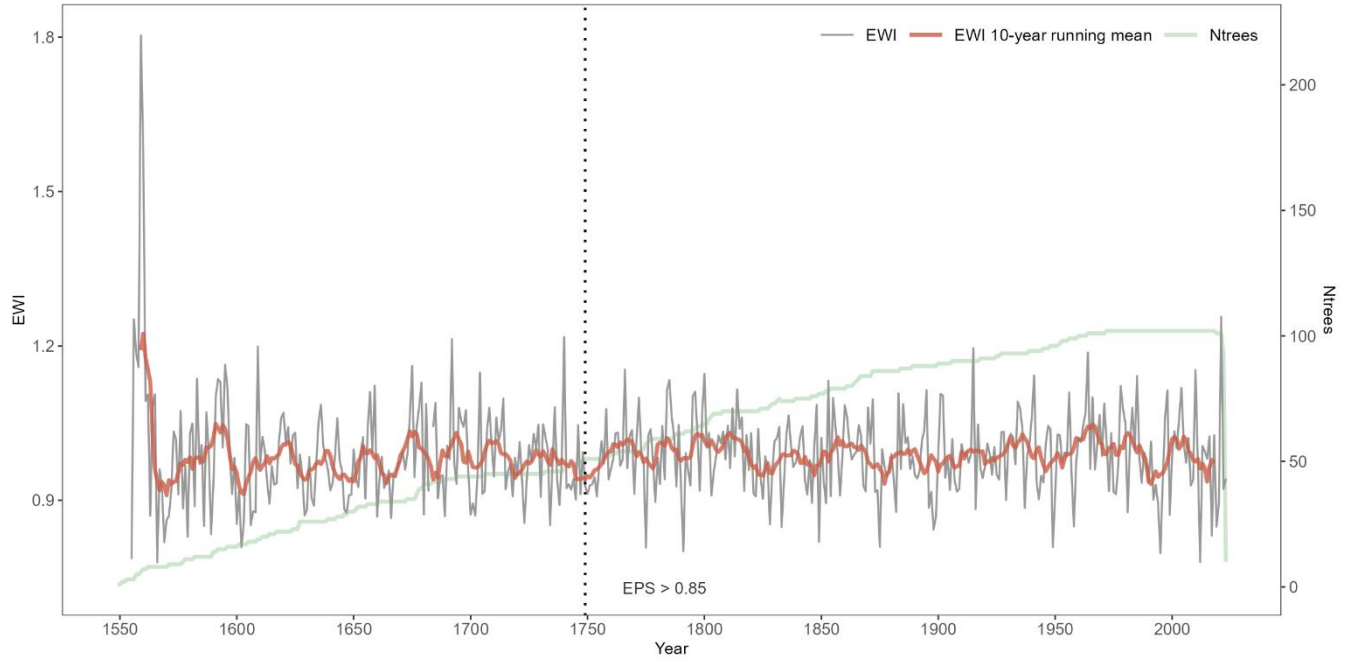

Figure S2: EWI chronology and sample depth.

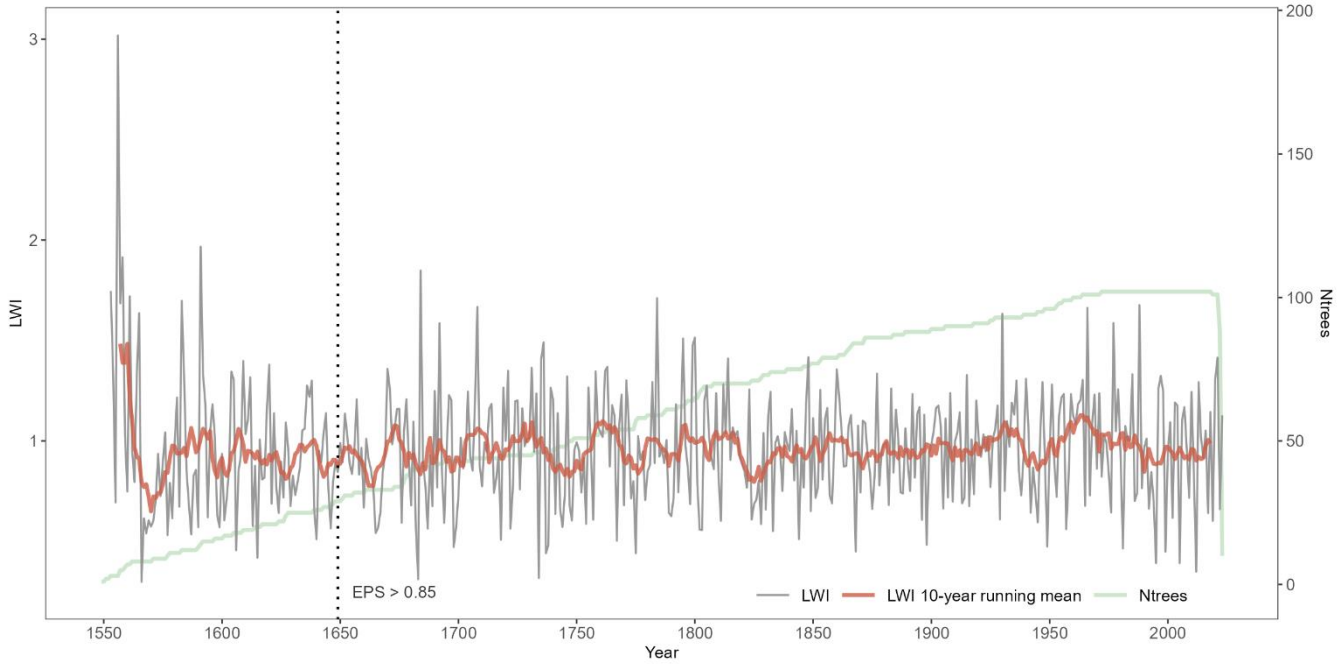

Figure S3: LWI chronology and sample depth.

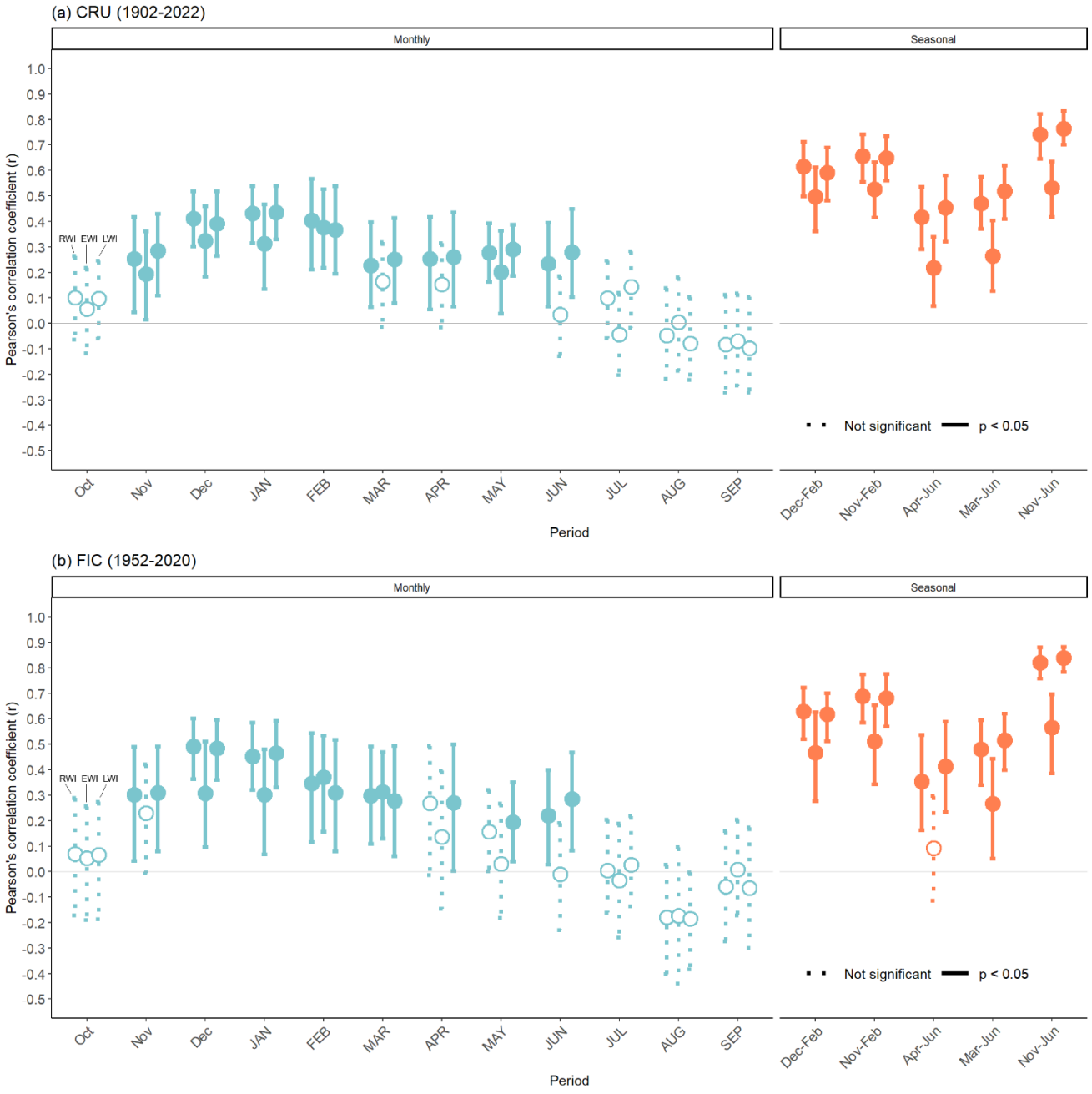

Figure S4: Monthly and seasonal Pearson's R correlations between site chronologies (RWI, EWI and LWI) and (a) CRU precipitation (1902–2022) or (b) FIC precipitation (1952–2020). Months in lowercase refer to the previous year, while those in uppercase correspond to the current year.

50

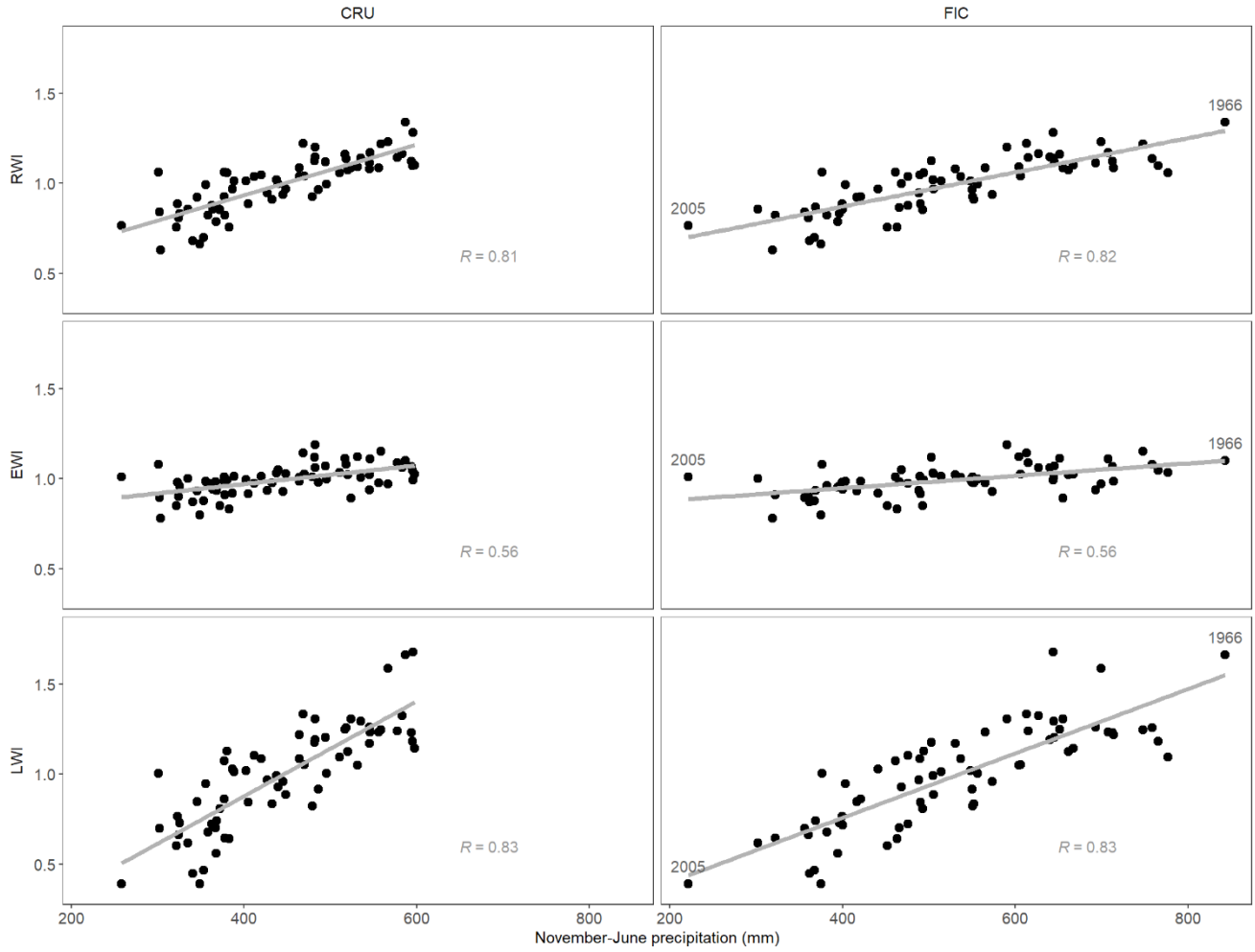

Figure S5: Scatterplots showing the November–June precipitation signal in site chronologies for RWI (top), EWI (middle), and LWI (bottom). Left panels use CRU precipitation data; right panels use FIC precipitation data. All correlations are computed over the common period covered by both datasets (1952–2020).

55

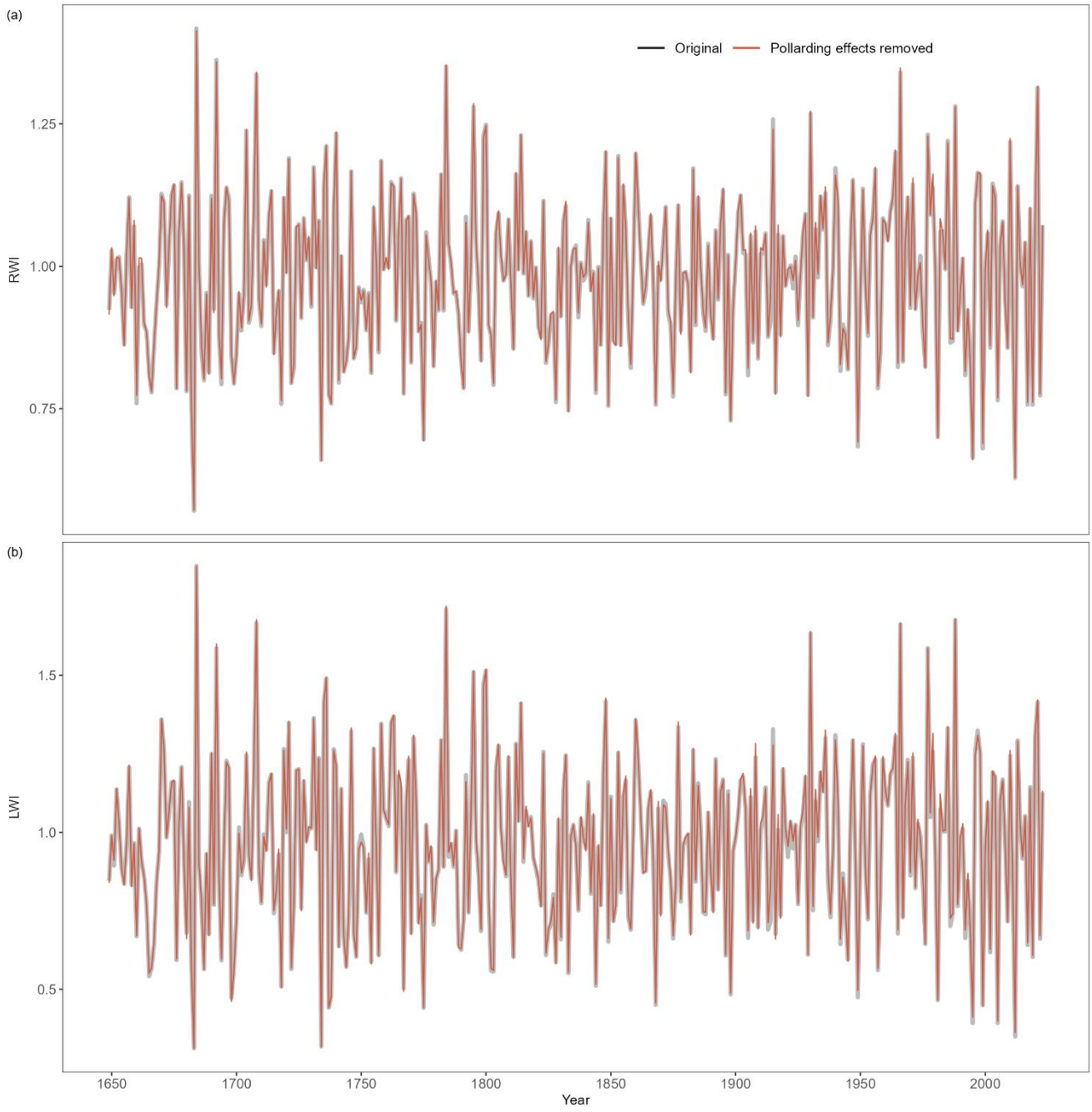

Figure S6: Comparison of RWI (a) and LWI (b) site chronologies before and after removing pollarding effects.

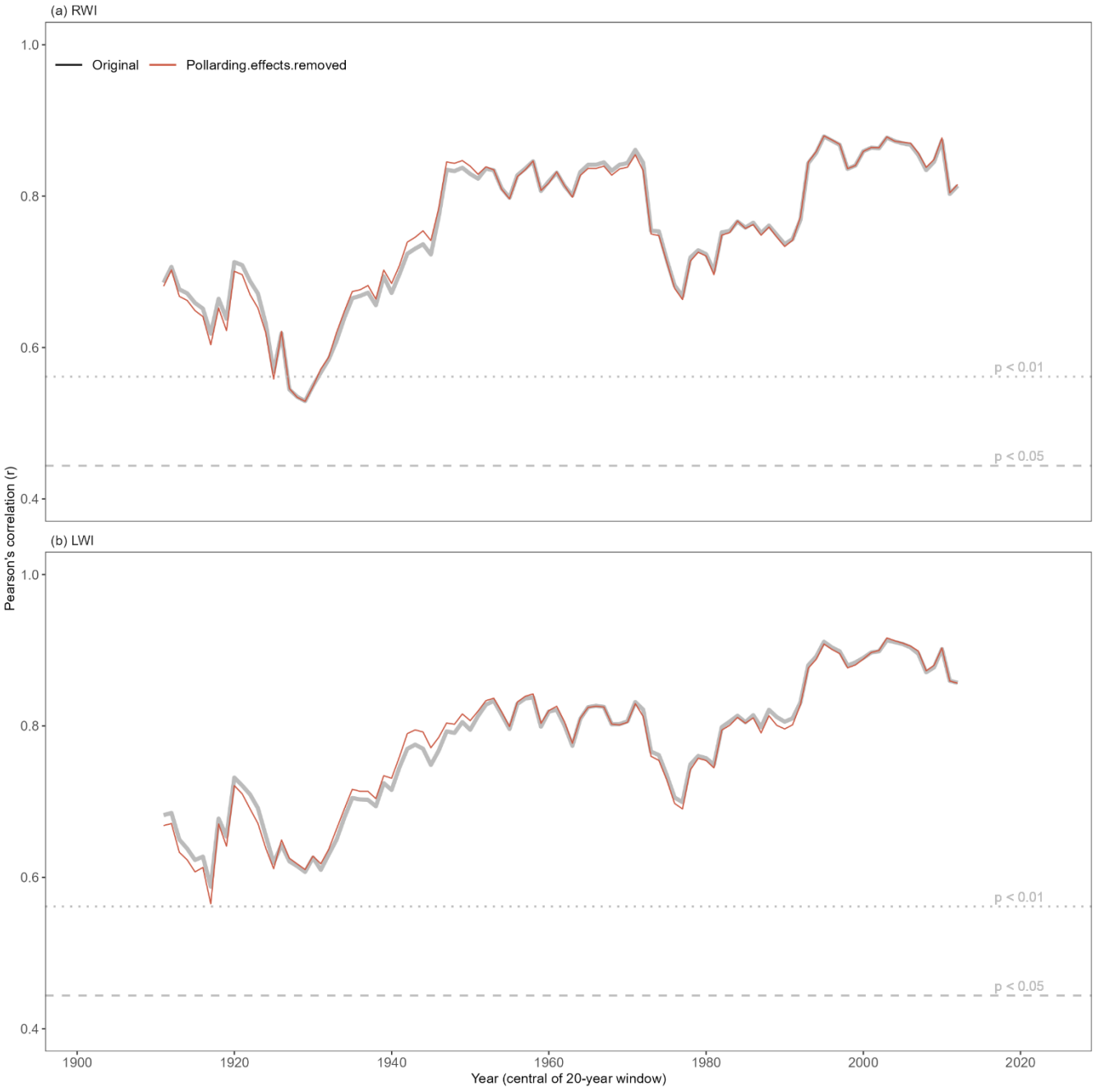

Figure S7: Stability of the dendroclimatic relationship between November–June precipitation and site chronologies before and after removing the effects of pollarding. Precipitation data source: CRU (1902–2022). Panels show RWI (a) and LWI (b) data. Pearson's R was calculated using a 20-year moving window.

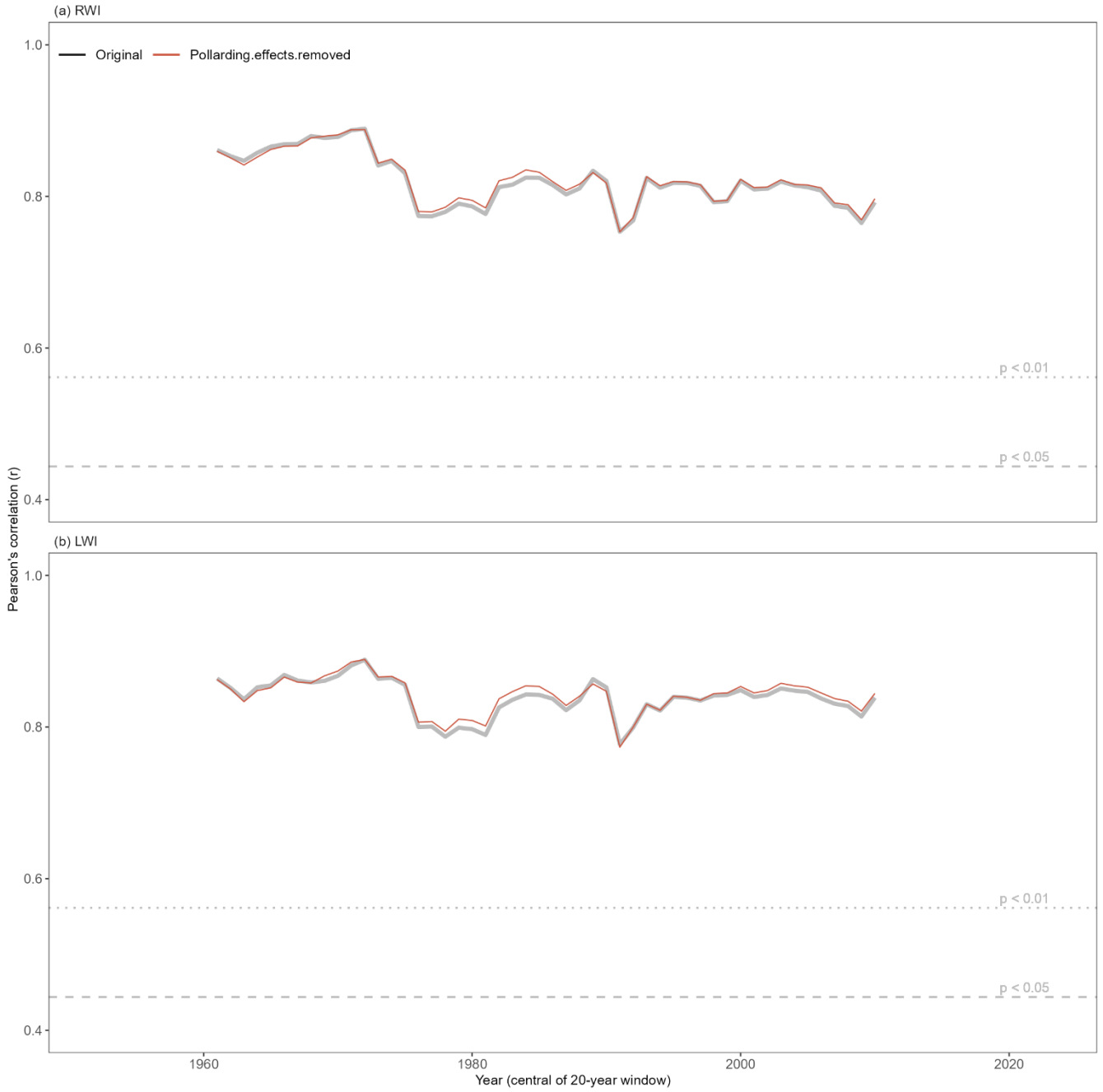

Figure S8: Stability of the dendroclimatic relationship between November–June precipitation and site chronologies before and after removing the effects of pollarding. Precipitation data source: FIC (1952–2020). Panels show RWI (top) and LWI (bottom). Pearson's R was calculated using a 20-year moving window.

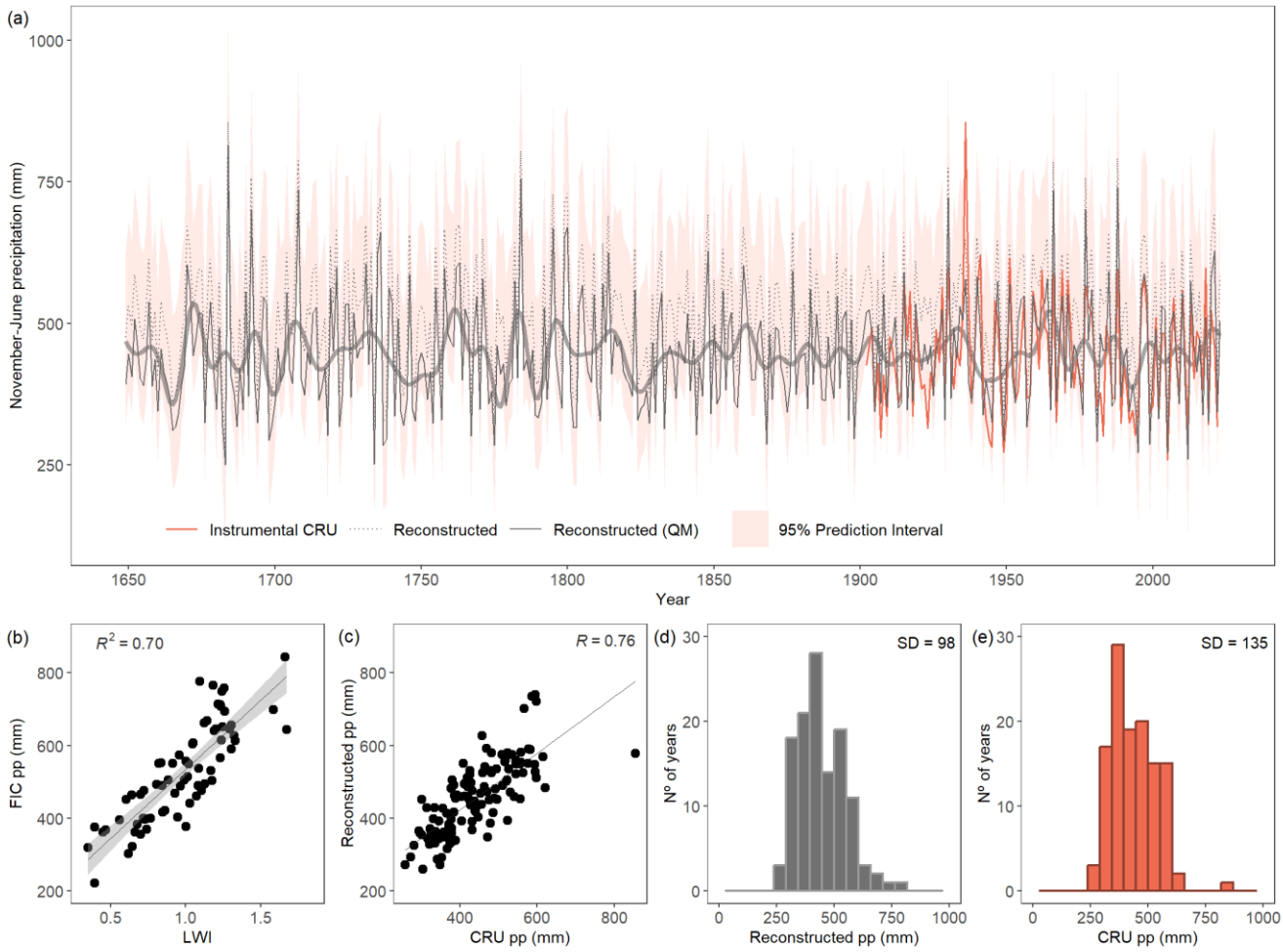

Figure S9: (a) Reconstructed November–June precipitation from 1649 to 2023 derived from pollarded oak LWI data in northcentral Spain, including the bias-corrected reconstruction (QM). Grey curves show interannual variability; the shaded area represents the 95% prediction interval of the final calibration model using the full FIC precipitation series (1952–2020). A band-pass filter was applied to isolate low-frequency variability by retaining periodicities between 10 and 100 years (thick line). The reconstruction is compared with full CRU precipitation series (1902–2022; orange line) to assess its consistency (Fig. 6 shows a split calibration–validation approach). (b) Scatterplot with linear regression between the LWI chronology and full FIC precipitation (1952–2020; final calibration). (c) Scatterplot showing the relationship between full CRU and the bias-corrected reconstruction (1902–2022). (d–e) Frequency distributions of bias-corrected reconstructed and full CRU precipitation, respectively (1902–2022).